An Approach for Pit Pattern Recognition in Colonoscopy Images

Veska Georgieva[1], Szilvia Nagy[2], Andras Horvath[3], Elena Kamenova[4]

[1,4]Technical University of Sofia, Bulgaria,
[2,3]SzechenyiIstvanUniversity of Györ, Hungary
vesg@tu-sofia.bg, nagysz@rs1.sze.hu,horvatha@sze.hu,elena.kamenova@best.eu.org

Abstract

In this worka new multistage approach is proposed for pit pattern recognition and classification of colonicmucosa, based on Kudoetal. Classifications system. Itconsistsoffollowingstages: narrow band (NB) colonoscopy image enhancement, binary transformation by adaptive threshold and shape recognition for obtaining pit contours. Thenthe best match for each pit contour is found by comparing each contour of the examined image with all the contours that are contained in the training sets by using Hu-moments algorithm.Finally, each pit appears outlined in a different colour according to its recognised type and each pit area is calculated.The ratio neopastic to non-neoplastic lesions is calculated for obtaining information about dangerous cases, which need immediate medical attention.The basic advantages of the proposed method are better quality of the processed image and the simple and faster algorithmfor pit pattern classification. It would help the physician by faster and more accurate recognition of colorectal cancer and to choosetherighttreatmentaccording to therespectivestage.In the paper are given also some results obtained by computer simulation of the proposed algorithm, applied on real NB images.

Keywords: *Narrow band images enhancement, pit pattern recognition, Kudo's classifications system, Hu-moments algorithm.*

1. Introduction

Narrow band imaging (NBI) is a technique of special light observation that enhances the visualisation of the capillary network and mucosal morphology during endoscopic observation of the gastrointestinal tract.Itusesscattering and absorption properties of human tissue.The penetration depth before being scattered (partly absorbed) depends on the wavelength of the light. The shorter wavelength (e.g. blue) is reflected. Longer wavelengths (e.g. green) penetrate deeper. The image obtained through white light is a composition of slightly different tissue layers. The result is an image with focus on superficial mucous layers (blue 415 nm) and the capillary network of the deeper submucosal layer (green 540 nm). A bright but partially blurred image is the result. Figure (1) presents different wavelength light and the mucosa [1].

NBI is useful for differentiating small colorectal non-neoplastic from neoplastic polyps and is highly accurate for distinguishing low-grade dysplasia from high-grade dysplasia/invasive cancer and can thus be used to predict the histopathology of colorectal neoplasia [2,3]. NBI colonoscopy is a procedure that would rather enhance vessels and the corresponding pit pattern than enhance the height of the mucosa.The fact that only selected bandwidths are emitted results in a lower brightness which requires special high-sensitive dual mode CCDs. Recent systems try to achieve such high contrast image depiction from post-processing using special software algorithms [4, 5]. A colorectal polyp is an abnormal protrusion of the mucosa in the bowel lumen that is classified by histopathological examination. Adenomas are a common finding during colonoscopy in symptomatic patients and in asymptomatic individuals undergoing screening.

If most polyps are small, it is well recognized that the risk of malignant transformation increases with increasing polyp size.Using NBI observation to analyze micro vessel visibility, vascular diameter and distribution heterogeneity, and the presence and irregularity of pit-like pattern, makes it possible to discriminate colorectal lesions as tumor versus, non-tumor and adenoma versus carcinoma.

Various classification and evaluation methods have been proposed on this base [6, 7, 8]. In the routine practicetechniques should be used that enhance surface and vascular patterns of colorectal lesions.

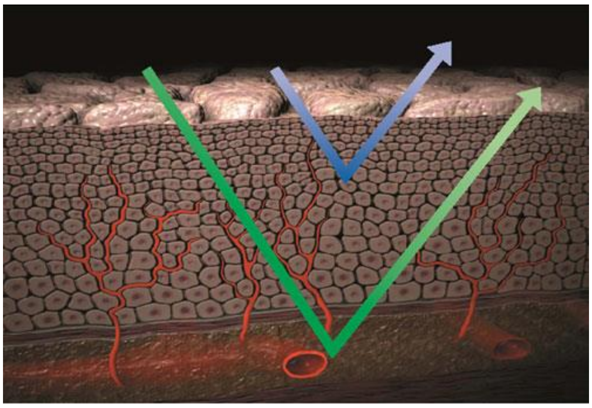

Figure (1): Different wavelengthlight and the mucosa

In this papera multistage approach is presented for NB colonoscopy imagesprocessing for obtaining a better visual quality and pit pattern recognition and classification of colonic mucosa, based on Kudo et al. classifications system.

The paper is arranged as follows: basic stages of the proposed algorithm for preprocessing and pit pattern recognition of NB images, presentation of some results, obtained by the simulation, and conclusions.

2. Basic stages of pit pattern recognition in NB images

The algorithm for pit pattern recognition in NB images comprises the following basic stages:

1) Preprocessing of NB image, which includes homomorphic filtering based on wavelet packet transformation as a first step of improving, and contrast limited adaptive

histogram equalization (CLAHE) as a second improving step to adjust its whole luminousness;

2) Selection of ROI image;

3) Binarization based on adaptive thresholding;

4) Recognition and classification of pit pattern;

5) Calculation of ratio of neoplastic and non-neoplastic pits.

2.1. Preprocessing stage

Image preprocessing is performed in order to reduce or eliminate noise and enhance the visual quality.

Homomorphic filtering (HF) can eliminate non-uniformity luminance distribution of image, and keep its original state. However, the property of local spatial domain has not been considered. As a result, enhancement in local contrast is poor. Moreover, the operational speed with the method of homomorphic filtering based on Fourier transformation is relatively slower, and it takes up more operational time and space [9].

Because of its individual characteristics, such as multiscale, spatial localization and frequency localization, wavelet transformation was used instead of Fourier's to improve operational efficiency. Then histogram equalization could be done on the image in order to increase its local contrast [10].

What is presented in our work is an approach for NB images enhancement using improved homomorphic filtering, based on wavelet packet transformation (WPT) [11]. Figure (2) shows the flowchart of the basic algorithm for preprocessing stage.

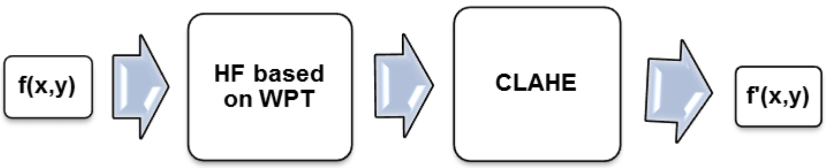

Figure (2): Flowchart of basic algorithm for preprocessing stage

The homomorphic filtering uses the illumination-reflectance model in its operation. The model presenting the image is characterized by two primary components. The first component is the amount of source illumination incident on the scene being viewed $i(x,y)$. The second component is the reflectance component of the objects on the scene $r(x,y)$. The image $f(x,y)$ is then defined as [12]:

$$f(x, y) = i(x, y).r(x, y) \qquad (1)$$

The intensity of $i(x, y)$ changes slower than $r(x, y)$. Therefore, $i(x,y)$ is considered to have lower frequency components than $r(x,y)$. Using this fact, homomorphic filtering technique aims to reduce the significance of $i(x,y)$ by reducing the low frequency components of the image. This can be achieved by executing the filtering process in the frequency domain. However, before the transformation takes place, a logarithm function has been used to change the multiplication operation of $r(x, y)$ with $i(x, y)$ in Eq.(1) into an addition operation.

$$z(x,y) = \ln f(x,y) = \ln i(x,y) + \ln r(x,y) \quad (2)$$

The improved homomorphic filtering schema is shown on Figure (3), where WPT is 2D Discrete Wavelet Packet Transformation, H(u,v) presents a filter function, IWPT is 2D Inverse Discrete Wavelet Packet Transformation and *g(x,y)* is the output image. The method can propose a more complete analysis and provides increased flexibility according to DWT. It has the following important properties:

- A richer presentation of the image, based on functions with wavelet forms, which consist of 3 parameters: position, scale and frequency of the fluctuations around a given position;
- Numerous decompositions of the image, that allows to estimate the noise reduction of different levels of its decomposition;
- Adaptive noise reduction on each level of the decomposition by choice of the best tree decomposition and optimal thresholds parameters.

Because the noise of wavelet transformation usually concentrates on the state of high resolution, the method is useful to reduce the noise.

Figure (3): Flowchart of improved homomorphic filtering

The filtration is obtained on the basis of the best shrinkage wavelet packet decomposition and the spatial adapted threshold that allows to determine the threshold in three directions: horizontal, vertical and diagonal [13].The wavelet thresholding procedure removes noise by thresholding only the wavelet coefficients of the detail sub-bands, while keeping the low resolution coefficients. In addition the threshold can be hard or soft. In addition, it is proposed to use the Normal Shrink method to calculate the threshold value only for the detail sub-bands in the best shrinkage decomposition. The scheme for obtaining the wavelet packet decomposition (WPD) for noise reduction is shown on Figure (4).

Figure (4): Schemeforobtainingthe WPD fornoisereduction

All these elements of the procedure for noise reduction can be determined on the basis of the calculated estimation parameters. PSNR and effectiveness of filtration (E_{FF}) values are higher for better denoised image where the value of noise reduction ratio (NRR) is lower.

CLAHE does not operate on the whole image. It works like an ordinary Histogram Equalization (HE), but on small areas it works in images, named tiles. Each tile's contrast is enhanced, so that the histogram of the output area roughly matches the histogram determined by the 'Distribution' parameter. The adjacent tiles are then combined using bilinear interpolation to eliminate artificially induced boundaries. The algorithm CLAHE limits the slope associated with the gray level assignment scheme to prevent saturation. This process is accomplished by allowing only a maximum number of pixels in each of the bins associated with the local histograms. After “clipping” the histogram, the clipped pixels are equally redistributed over the whole histogram to keep the total histogram count identical.

The procedures noise reduction and CLAHE are applied to a selected image, processed in YUV system for more effectiveness.

2.2. Selection of ROI image

Selection of ROI image is performed in order to analyse the interesting area of the investigated image. It can be made interactivewith the mouse from the doctor.

2.3. Binarization based on adaptive thresholding

First, selected ROI images are converted to grayscale. In order to account for variations in illumination, which is typical for the colonoscopy images,the common solution is adaptive thresholding. This method can calculate the threshold for every small region in the image. We get different thresholds for different regions of the same image and it gives us better results for images with varying illumination. In this case the threshold value is the weighted sum of neighbourhood values where weights are a Gaussian window [14].

Too small and isolated contours are defined as false contours. They are found andremoved by a second threshold step. In this case morphological dilatation and erosion are not applied because this can present the contours with unnatural edges.

2.4. Recognition and classification of pit pattern

As afirst step a detection of all contours of pits on the imageis made. As next, thematchShape methodbased on Hu’s moments is used to find the best match from the training set images for each contour of the image [15, 16]. The basic idea of this method is to describe the objects by a group of features which provide discrimination power to identify objects from differentgroups.The moment invariants have been proved to be the adequate measures for tracing image patterns regarding the images translation, scaling and rotation. In addition a number that indicates the similarity between the shapes can be returned. The lower the number, the better the match is. There are 3 different variations, each using the Hu invariants. The suitable variant can be chosen byexperiment. We choose the third variant because it is more suitable to complex shapes such as pit pattern types.

For classifying the pit patterns, the system, developed by Kudo [17] was used. Originally it is based on 6 types of patterns, as described on Figure (5) [18]. But in real life classification is not really that easy.For the developed method, types III-s and V are not included. Type III-s is too small to be accurately detected and gets mixed with image noises. Type V, as described in [17] is a combination of types III-L and IV pits. As each pit is being processed separately, they are being classified as either type III-L or IV and thus using type V becomes pointless.

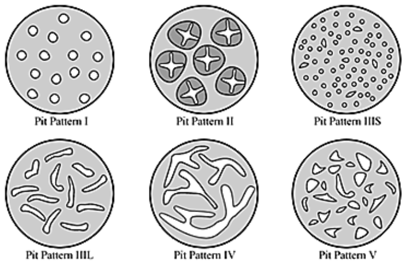

Pit pattern type	Characteristics
I	roundish pits
II	stellar or papillary pits
III S	small roundish or tubular pits (smaller than type I pits)
III L	large roundish or tubular pits (larger than type I pits)
IV	branch-like or gyrus-like pits
V	non-structured pits

Figure (5): Different pit pattern types and their characteristics

As next a colour is assigned to each finding type in the output images.Types I and II, being not malicious and not requiring immediate interference, appear respectively in green and blue. The dangerous III-s and IV types are shown respectively in dark-red and red.

2.5. Calculation of ratio of neoplastic and non-neoplastic pits

This number is calculated by first finding the active area of the picture (non-black or non-empty pixels) and then calculating the area covered by pits from each type. The final ratio is the coefficient of the sum of types III-s and IV areas and the sum of types I and II type areas. The higher the number, the bigger amount of dangerous pits is presented on the image.

3. Experimental Results

For the experiments were used real NB images of the image database of the Medical Academy Sofia and Petz Aladár Hospital Győr. A part of the experimental results is given below. The formulated stages of preprocessing are presented by computer simulation in MATLAB, version 8.1 environment. The stages needed for pit pattern recognition are simulated in Python environment and OpenCV functions. In analysis are used 30 NB images with size 768x576 from colonoscopy. They are divided into 3 sets (groups) of similar images regarding the colonic mucosa. Each group comprises N=10 NB images. The original images have been done in jpeg file format. By preprocessing they are converted in YUV system and bmp format.

Figure (6) shows 3 NB images and their modifications obtained by substages of preproocessing, which represent the three different groups of similar images regarding the colonic mucosa. The ROI images selected after preprocessing are presented on Figure (7).

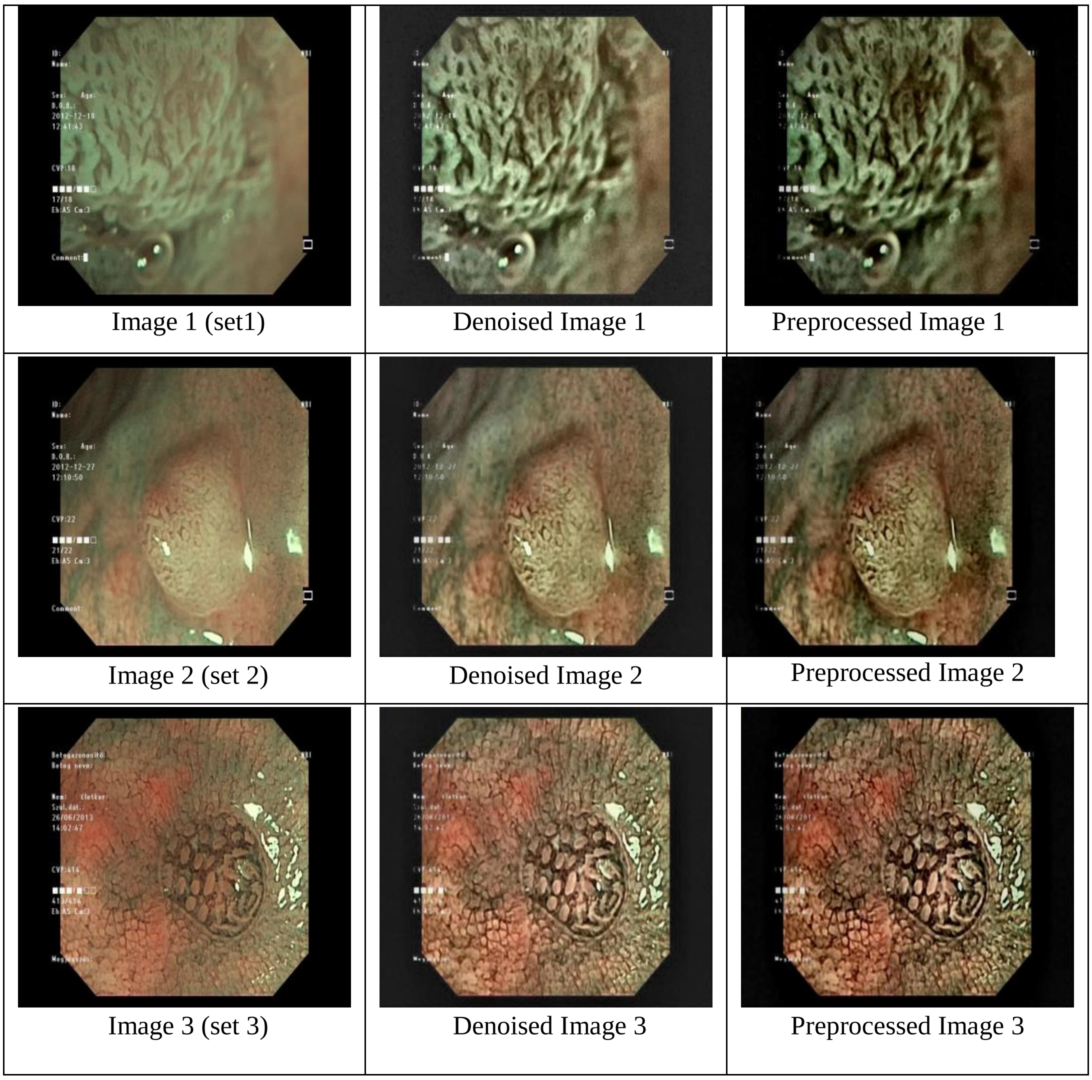

Figure(6):Original NB images and their modifications, obtained as a result of preprocessing stage

a) b) c)

Figure (7): Selected ROI of the preprocessed NB images: a) image 1; b) image 2; c) image 3

In Figure (8) is given a graphical presentation of number of errors obtained by each of the matchShape options. The comperative analysis has shown that the third method is more suitable in the case of pit pattern.

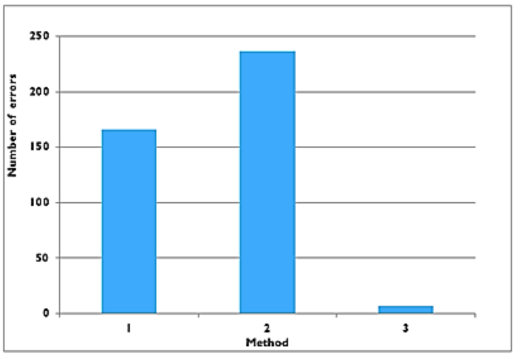

Figure (8): Number of errors, obtained by different options for Hu' moment invariants

Some results obtained by simulation are shown in Table 1. They give information about the pit pattern recognition and classification in investigated ROI images and the neo plastic to non-neoplastic ratio. A visual presentation of the obtained results for pit pattern recognition in the original and preprocessed three ROI images are given in Figure (9).

Table 1.Pit pattern recognition and neo plastic to non-neoplastic ratio in original and processed ROI images in %

ROI images	Type I	Type II	Type III-L	Type IV	R
Original image 1	0.57	8.24	9.44	22.55	3.63
Processed image 1	0.49	0.11	6.83	27.63	4.95
Original image 2	2	4.69	10.45	2.28	1.90
Processed image 2	2.81	6.12	4.64	37.79	4.75
Original image 3	0	72.98	2.06	6.82	0.12
Processed image 3	0.11	10.93	21.65	15.08	3.33

Figure (10) gives graphical interpretation of neoplastic to non-neoplastic ratio in the all 10 images from set 1 in percents. The obtained results for neoplastic to non-neoplastic ratio from the other two sets of images are similar.

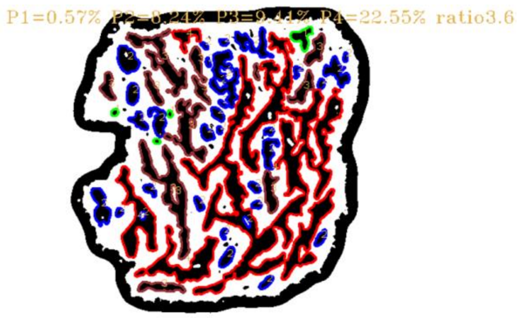 Pit pattern recognition of original ROI image 1	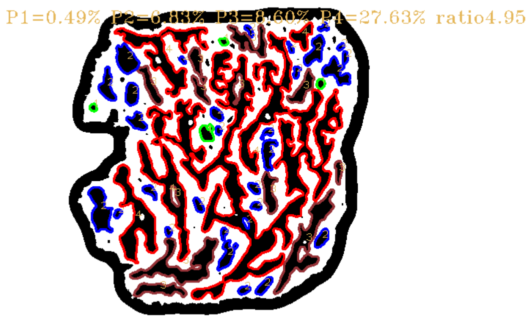 Pit pattern recognition of processed ROI image 1
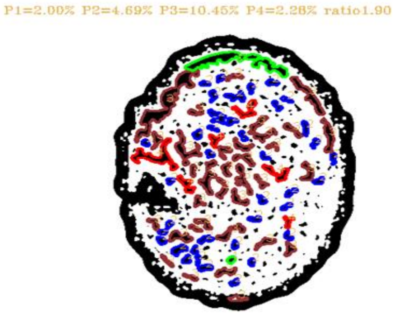 Pit pattern recognition of original ROI image 2	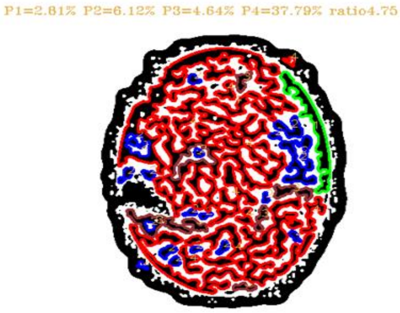 Pit pattern recognition of processed ROI image 2
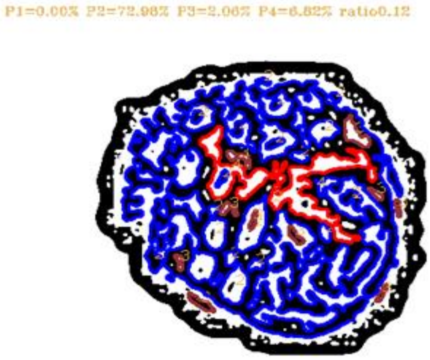 Pit pattern recognition of original ROI image 3	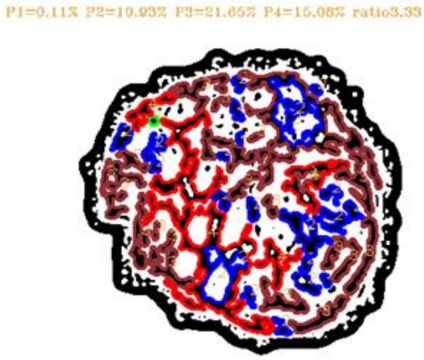 Pit pattern recognition of processed ROI image 3

Figure (9): Pit pattern recognition of ROI images

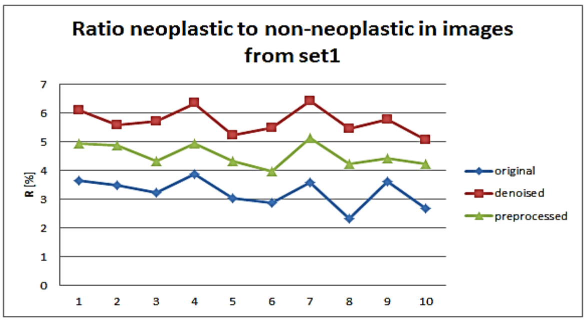

Figure (10): Calculated R [%] in original, denoised and preprocessed ROI images from set 1

The implemented studying and obtained experimental results have shown that the original ROI images have a bad quality and the recognition of the different pit pattern is difficult. The images obtainbetter quality by noise reduction, but some very fine contours of pit pattern can be lost, the area of neoplastic regions grows and the neoplastic to non-neoplastic ratio will be much higher. After contrast enhancement, which is the last stage of preprocessing, pit patterns have well-defined outlines and neoplastic to non-neoplastic ratio is more precise.

4. Conclusions

In the paper we propose a new multistage approach for pit pattern recognition and classification of the colonic mucosa, based on Kudo et al. classifications system. The basic advantages are obtaining better quality of the processed image and the simple and faster algorithm for pit pattern classification. This approach can be very useful by colorectal screenings, for the easy detecting of early colorectal carcinoma and monitoring of disease progression. The implemented algorithm provides a basis for further investigations in more precise polyp surface segmentation.

Acknowledgements

The authors are exceptionally grateful to Professor Dr. V. Hadjidekov and Dr. Genov at the Department of Image Diagnostic on the Medical Academy in Sofia and Professor István Rácz and his group at the Department of Gastroenterology at the Petz Aladár County Educational Hospital for the images and advice for the investigations.

References

[1]. H. Dremel,"General Principles of Endoscopic Imaging", Principles and Practice of Interventional Pulmonology, Springer Media New York, 15- 25, 2013.

[2]. Y. Sano, H. Ikematsu, K. Fu et al., "Meshed capillary vessels by use of narrow-band imaging for differential diagnosis of small colorectal polyps," *Gastrointestinal Endoscopy*, Vol. 69, no. 2, 278–283, 2009.

[3]. A. Katagir, K, Fu, Y. Sano et al., "Narrow band imaging with magnifying colonoscopy as diagnostic tool for predicting histology of early colorectal neoplasia," *Alimentary Pharmacology and Therapeutics*, vol. 27, no. 12, 1269–1274, 2008.

[4]. W. Kage, S. Mühldorfer, T. Bergen, C. Münzenmayer, T. Wittenberg, “The importance of image quality assessment for the creation of reference image collection for computer-assisted diagnosis in colonoscopy”, In Int J CARS (2013) 8 (Suppl 1): S405-S406, Heidelberg, 2013.

[5]. M. Häfner, C. Kendlbacher, W. Mann, W. Taferl, F. Wrba, A. Gangl, A. Vecsei, and A. Uhl, “Pit pattern classification of zoom-endoscopic colon images using histogram techniques,” in Proc of the 7th NordicSignal Processing Symposium (NORSIG’06), pp. 58–61, 2006.

[6]. D.P. Hurlstone et al. “Efficacy of high magnification chromoscopic colonoscopy for the diagnosis of neoplasia in flat and depressed lesions of the colorectum: a prospective analysis”, *Gut* , 53:284–290, 2004.

[7]. K. Konishi et al. “A comparison of magnifying and nonmagnifying colonoscopy for diagnosis of colorectal polyps: a prospective”, Gastrointestinal Endoscopy, 57:48–53, 2003.

[8]. Kanao H, Tanaka S, Oka S, Kaneko I, Yoshida S, Arihiro K, Yoshihara M, Chayama K., ”Clinical significance of type VI pit pattern subclassification in determining the depth of invasion of colorectal neoplasms”, World J Gastroenterol, 14(2): 211-217, 2008.

[9]. Wen Sha, You Zhi-sheng, “A performance optimized algorithm of spatial domain homomorphic filtering,” Application Research of Computers, Vol.173, 62-65, 2000.

[10]. Wenli Liu, Peng He, Hui Li, Hongbo YuH.,” Improvement on the Algorithm of Homomorphic Filtering”, Advances in Biomedical Engineering, Vol.11, 120- 124, 2012.

[11]. V. Georgieva, “Homomorphic filtering approach for narrowband images enhancement”, Journal of Applied Electromagnetism (JAE), in print.

[12]. C.-N. Fan and F.-Y. Zhang, "Homomorphic filtering based illumination normalization method for face recognition," Pattern Recognition Letters, vol. 32, pp. 1468-1479, 2011.

[13]. V.Georgieva, R.Kountchev, “An influence of the wavelet packet decomposition on noise reduction in ultrasound images”, Proceedings of International Scientific Conference on Information, Communication and Energy Systems and Technology, pp.185-188, Sofia, Bulgaria, 2006.

[14]. Rafael C. Gonzalez and Richard E. Woods, Digital Image Processing, prentice Hall, 2nd edition, 2002.

[15]. Huang, Z., Leng, J. “Analysis of Hu’s Moment Invariants on Image Scaling and Rotation”, Proceedings of the 2nd International Conference on Computer Engineering and Technology (ICCET). pp. 476-480, 2010.

[16]. Ming Kuei-Hu, “Visual Pattern Recognition by Moment Invariants”, IRE Transactions on Information Theorie, 8:179-187, 1962.

[17]. S Kudo, S Hirota, T Nakajima, S Hosobe, H Kusaka, T Kobayashi, M Himori, and A Yagyuu, “Colorectal tumours and pit pattern”. J Clin Pathol., Oct; 47(10): 880–885, 1994.

[18]. M. Häfner, et al. „Pit pattern classification using multichannel features and multiclassification” in Handbook of research on advanced techniques in diagnostic imaging and biomedical applications, Information Science Reference (an imprint of IGI Global), Hershey, USA, 2009